

Analytical Characterization of the Accuracy of SLAM without Absolute Orientation Measurements

Anastasios I. Mourikis and Stergios I. Roumeliotis

Dept. of Computer Science & Engineering, University of Minnesota, Minneapolis, MN 55455

Email: {mourikis|stergios}@cs.umn.edu

Abstract—In this paper we derive analytical upper bounds on the covariance of the state estimates in SLAM. The analysis is based on a novel formulation of the SLAM problem, which enables the simultaneous estimation of the landmark coordinates with respect to a robot-centered frame (relative map), as well as with respect to a fixed global frame (absolute map). A study of the properties of the covariance matrix in this formulation yields *analytical* upper bounds for the uncertainty of both map representations. Moreover, by employing results from Least Squares estimation theory, the *guaranteed accuracy* of the robot pose estimates is derived as a function of the accuracy of the robot’s sensors and of the properties of the map. Contrary to previous approaches, the method presented here makes no assumptions about the availability of a sensor measuring the absolute orientation of the robot. The theoretical analysis is validated by simulation results and real-world experiments.

I. INTRODUCTION

Recent interest in Simultaneous Localization and Mapping (SLAM) has resulted in significant advances in the design of estimation algorithms [1]–[5], data association techniques [6], and sensor data processing [7], [8], which have enabled localization with maps consisting of millions of landmarks (e.g., [1]). However, a theoretical characterization of the attainable localization accuracy in SLAM remains an open problem to date. To the best of our knowledge, very few approaches exist in the literature that focus on *predicting* the accuracy of the robot’s pose and of the map estimates, given the capabilities of a robot’s sensor payload. As a result, evaluating the suitability of a robot with a given set of sensors for a particular SLAM application, largely remains a matter of exhaustive simulations and experimentation.

In this paper, we focus on deriving upper bounds for the covariance of the state estimates in SLAM, as a function of the accuracy of the robot’s sensors and the size of the map. The derived closed-form expressions provide *theoretical guarantees* for the accuracy of SLAM, and can thus be employed during the design of a localization system, to determine the necessary accuracy of the robot’s sensors. Contrary to previous approaches [9], [10], in the treatment presented here we do not assume that the robot is equipped with an absolute orientation sensor, and thus the problem formulation is more general. In order to derive analytical expressions for the upper bounds on the localization uncertainty, we employ a novel formulation of the SLAM problem, in which the landmark coordinates with respect to (i) the robot, and (ii) a fixed global frame, are jointly estimated. This enables us to compute upper bounds on the covariance of *both* map representations (cf. Section III), as well as on the uncertainty in the robot’s

pose (cf. Section IV). Before delving into the details of our approach, in the following section we present an overview of related work.

II. RELATED WORK

One of the first attempts to study the properties of the covariance matrix of the state estimates in SLAM was presented in [11]. In that work, a Linear Time Invariant (LTI) SLAM model is employed, in which both the robot and the landmarks are constrained to lie in a one-dimensional space. For this simple model, the solution to the Riccati differential equation, which describes the time evolution of the covariance matrix of the position estimates, is derived in closed form. This result demonstrates some of the properties of the covariance matrix in SLAM, but its practical importance is limited by the fact that the analysis holds only for motion in 1D. The work of [11] has been extended to the case of a team of multiple vehicles performing SLAM [12] under the same set of assumptions (i.e., LTI system model, and motion in 1D).

A different set of properties of the covariance matrix in SLAM is studied in [13]–[15]. In particular, it is shown that the covariance matrix of the landmarks’ position estimates is decreasing monotonically, as more observations are processed, and after sufficient time, the map estimates become fully correlated. Additionally, the authors derive a *lower bound* on the covariance matrix, by considering the case in which the odometry measurements are *perfect*. Since no additional uncertainty is introduced in the system during state propagation, this is the “best-case scenario”. The covariance of the state estimates in this hypothetical system defines a lower bound, which depends only on the initial uncertainty of the robot’s pose. These results are also extended to the case of *cooperative* Concurrent Mapping and Localization in [16], [17]. A limitation of the aforementioned approaches is that the derived lower bounds are *independent* of the accuracy of the robot’s sensors, and thus cannot be employed for *comparing* the performance of robots with sensors of different quality. Moreover, if the robot’s initial pose is perfectly known, which is a common situation in SLAM, these bounds are equal to zero, and are thus non-informative.

In [9], upper bounds on the uncertainty of the position estimates in SLAM, as closed-form functions of the accuracy of the robot’s sensors, are derived. This is achieved by assuming that the robot is equipped with an *absolute orientation* sensor (e.g., a compass). When such a sensor is available, the maximum variance of the orientation errors is bounded, and a position-only Extended Kalman Filter estimator can be

formulated. This work is extended to the case of Cooperative SLAM in [10], under the assumption that every robot has an absolute orientation sensor. Clearly, there exist cases where such a requirement is not satisfied. We here extend the results of our previous work to the case where no absolute orientation measurements are available, resulting in a more general formulation. As shown in Section IV, in SLAM it is possible to derive an upper bound on the variance of the robot's orientation errors, *without* requiring that a compass or similar sensor be available.

III. THE UNCERTAINTY OF MAP ESTIMATION IN SLAM

In this section, we derive upper bounds for the covariance of the landmarks' position estimates in SLAM. In particular, we compute upper bounds for the uncertainty of the landmarks' positions when these are expressed with respect to i) a fixed global frame (absolute map), and ii) the robot's coordinate frame (relative map).¹ Our approach is based on formulating an Extended Kalman Filter (EKF) estimator, in which the state vector is comprised of both the relative map coordinates, *and* the absolute map coordinates, but does *not* explicitly contain the robot pose. The estimate for the robot pose, as well as its covariance, can be inferred from the transformation between the two map representations, as shown in the following section.

We point out that the computational complexity of this formulation is higher than that of the standard EKF. However, the sole purpose of employing such a formulation of SLAM is to determine analytical upper bounds for the covariance of the state estimates. As will be made clear in the following, in the proposed EKF set-up *all* available measurements are used once, and apart from linearization, no other approximations are made. Therefore, the covariance of the absolute map computed with this filter will be identical (except for small linearization inaccuracies) to the covariance that is computed with the "traditional" EKF SLAM algorithm [18], in which the state vector contains the absolute map coordinates and the robot pose.

A. Relative-map SLAM

We first study the case in which the state vector is comprised only of the landmarks' positions with respect to the robot (relative map). Denoting the position of the i -th landmark with respect to the robot at time step ℓ by ${}^R p_{i_\ell}$, $i = 1 \dots N$, we obtain the state propagation equation:

$${}^R p_{i_{k+1}} = {}^{R_{k+1}} p_{R_k} + C(-\omega_k \delta t) {}^R p_{i_k} \quad (1)$$

where the rotation matrix expressing the rotation of the robot frame between time-steps $k+1$ and k is:

$$C(-\omega_k \delta t) = \begin{bmatrix} \cos(\omega_k \delta t) & \sin(\omega_k \delta t) \\ -\sin(\omega_k \delta t) & \cos(\omega_k \delta t) \end{bmatrix} \quad (2)$$

¹We note that the term "relative map" is used in this paper to describe a robot-centred map. This is different than the notion of the relative map employed, for example, in [13].

and ${}^{R_{k+1}} p_{R_k}$ is the position of the robot at time-step k , expressed with respect to the robot frame at time-step $k+1$:

$${}^{R_{k+1}} p_{R_k} = -C(-\omega_k \delta t) {}^{R_k} p_{R_{k+1}} = -v_k \delta t C(-\omega_k \delta t) e_1 \quad (3)$$

In the preceding expressions, v_k and ω_k are the translational and rotational velocity of the robot at time step k , respectively, δt is the sampling interval, and $e_1 = [1 \ 0]^T$.

Using the measurements of the robot's translational and rotational velocities, v_{m_k} and ω_{m_k} , respectively, the position estimate of the i -th landmark is propagated according to:

$$\begin{aligned} {}^R \hat{p}_{i_{k+1}} &= {}^{R_{k+1}} \hat{p}_{R_k} + C(-\omega_{m_k} \delta t) {}^R \hat{p}_{i_k} \\ &= C(-\omega_{m_k} \delta t) (-v_{m_k} \delta t e_1 + {}^R \hat{p}_{i_k}) \end{aligned} \quad (4)$$

By linearizing Eq (3), we obtain the error propagation equation for the relative position of the i -th landmark:

$$\begin{aligned} {}^R \tilde{p}_{i_{k+1}} &= C(-\omega_{m_k} \delta t) {}^R \tilde{p}_{i_k} - \delta t C(-\omega_{m_k} \delta t) e_1 \tilde{v}_k \\ &\quad + \delta t J_\times {}^R \hat{p}_{i_{k+1}} \tilde{\omega}_k \end{aligned} \quad (5)$$

In the last expression, the symbol $\tilde{\cdot}$ denotes the error in the estimate of the respective quantity, and

$$J_\times = \begin{bmatrix} 0 & 1 \\ -1 & 0 \end{bmatrix} \quad (6)$$

If we create a state vector, ${}^R \mathbf{X}$, comprised of the relative positions of the landmarks with respect to the robot, then the error propagation equation for this state vector is:

$${}^R \tilde{\mathbf{X}}_{k+1} = {}^R \Phi_k {}^R \tilde{\mathbf{X}}_k + {}^R \mathbf{G}_k n_{\text{od}} \quad (7)$$

where $n_{\text{od}} = [\tilde{v}_k \ \tilde{\omega}_k]^T$ is the noise of the robot's odometry measurements, assumed to be zero-mean, white Gaussian, with covariance matrix $Q = \text{diag}(\sigma_v^2, \sigma_\omega^2)$. The state transition matrix is given by²

$${}^R \Phi_k = I_N \otimes C(-\omega_{m_k} \delta t) \quad (8)$$

and ${}^R \mathbf{G}_k$ is a $2N \times 2$ block matrix, whose i -th element is

$$G_{i_k} = \delta t [-C(-\omega_{m_k} \delta t) e_1 \quad J_\times {}^R \hat{p}_{i_{k+1}}] \quad (9)$$

The covariance propagation equation for the uncertainty of the *relative map* is

$${}^R \mathbf{P}_{k+1|k} = {}^R \Phi_k {}^R \mathbf{P}_{k|k} {}^R \Phi_k^T + {}^R \mathbf{Q}_k \quad (10)$$

where we have denoted ${}^R \mathbf{Q}_k = {}^R \mathbf{G}_k Q {}^R \mathbf{G}_k^T$, and ${}^R \mathbf{P}_{k+1|k}$ and ${}^R \mathbf{P}_{k|k}$ are the covariance of the error in the state estimate of ${}^R \mathbf{X}(k+1)$ and ${}^R \mathbf{X}(k)$ respectively, after measurements up to time k have been processed.

²In the remainder of this paper, I_n denotes the $n \times n$ identity matrix, $\mathbf{1}_{n \times m}$ denotes the $n \times m$ matrix of ones, $\mathbf{0}_{n \times m}$ denotes the $n \times m$ matrix of zeros, and \otimes denotes the Kronecker product.

B. The Dual-Map Filter

In order to introduce the absolute landmark coordinates in the state vector, we begin with the observation that, without loss of generality, the global coordinate frame can be selected at the initial position of the robot. Thus, at the first time step, the absolute and relative maps *coincide*, i.e., ${}^G\mathbf{X} = {}^R\mathbf{X}_0$, where ${}^G\mathbf{X}$ is a vector that contains the coordinates of the N landmarks with respect to the fixed global frame. If at the first time step, we augment the state vector to include two identical copies of the state ${}^R\mathbf{X}_0$, and we thereafter propagate only one of the copies, while properly accounting for the correlations between the two, then at every time step an estimate for both the relative, and the absolute landmark coordinates will be available.

The augmented state vector is $\mathbf{X} = [{}^R\mathbf{X}^T \quad {}^G\mathbf{X}^T]^T$, and the error-state propagation equation is given by

$$\begin{aligned}\tilde{\mathbf{X}}_{k+1} &= \begin{bmatrix} {}^R\Phi_k & \mathbf{0}_{2N \times 2N} \\ \mathbf{0}_{2N \times 2N} & I_{2N} \end{bmatrix} \tilde{\mathbf{X}}_k + \begin{bmatrix} I_{2N} \\ \mathbf{0}_{2N \times 2N} \end{bmatrix} {}^R\mathbf{G}_k n_{od} \\ &= \Phi_k \tilde{\mathbf{X}}_k + \mathbf{G} {}^R\mathbf{G}_k n_{od}\end{aligned}\quad (11)$$

while the covariance propagation equation is given by

$$\mathbf{P}_{k+1|k} = \Phi_k \mathbf{P}_{k|k} \Phi_k^T + \mathbf{G} {}^R\mathbf{Q}_k \mathbf{G}^T \quad (12)$$

Immediately after state duplication, and before the robot starts moving, the two copies of the state carry exactly the same information, and are thus fully correlated. As a result, the initial covariance matrix for the augmented state vector is given by:

$$\mathbf{P}_{0|0} = \begin{bmatrix} {}^R\mathbf{P}_{0|0} & {}^R\mathbf{P}_{0|0} \\ {}^R\mathbf{P}_{0|0} & {}^R\mathbf{P}_{0|0} \end{bmatrix} \quad (13)$$

At every time step, the robot performs a direct observation of the *relative positions* of all landmarks, and therefore the measurement vector at each time step is described by

$$\mathbf{z}(k) = \mathbf{H}\mathbf{X}_k + \mathbf{n}(k), \quad \text{with } \mathbf{H} = [I_{2N} \quad \mathbf{0}_{2N \times 2N}] \quad (14)$$

where $\mathbf{n}(k)$ is a Gaussian, zero-mean, white noise vector. The measurements of different landmarks are independent, and therefore the covariance matrix of $\mathbf{n}(k)$ will be a generally time-varying, block-diagonal matrix:

$$\mathbf{R}_k = \text{Diag}(R_{i_k}) \quad (15)$$

where R_{i_k} is the 2×2 covariance matrix of the measurement of the i -th landmark. Using these definitions, we can write the covariance update equation of the EKF as:

$$\mathbf{P}_{k+1|k+1} = \mathbf{P}_{k+1|k} - \mathbf{P}_{k+1|k} \mathbf{H}^T \mathbf{S}_{k+1}^{-1} \mathbf{H} \mathbf{P}_{k+1|k} \quad (16)$$

with $\mathbf{S}_{k+1} = \mathbf{H} \mathbf{P}_{k+1|k} \mathbf{H}^T + \mathbf{R}_{k+1}$.

At this point, a clarification regarding the structure of the measurement equation (cf. Eq. (14)) is due. At first, the fact that the measurement equation does not directly involve the absolute position estimates of the landmarks may appear somewhat peculiar. Note, however, that the close relation existing between the absolute and relative maps is expressed via the correlations in the augmented system covariance matrix.

These correlations ensure that, during each EKF update step, the absolute map estimates as well as their covariance are appropriately corrected.

By combining the covariance propagation and update equations (Eqs. (12) and (16)), we form the Riccati recursion that describes the time evolution of the covariance matrix in the augmented system. This is given by:

$$\mathbf{P}_{k+1} = \Phi_k (\mathbf{P}_k - \mathbf{P}_k \mathbf{H}^T \mathbf{S}_k^{-1} \mathbf{H} \mathbf{P}_k) \Phi_k^T + \mathbf{G} {}^R\mathbf{Q}_k \mathbf{G}^T \quad (17)$$

where we have introduced the substitutions $\mathbf{P}_k = \mathbf{P}_{k+1|k}$ and $\mathbf{P}_{k+1} = \mathbf{P}_{k+2|k+1}$ to simplify the notation.

In this paper, we consider the case where the landmark positions are *unknown* prior to the first observation, and the robot has perfect initial knowledge of its pose, which is the most common setting for SLAM. Immediately after the first set of robot-to-landmark measurements, the uncertainty of the relative map is equal to the covariance matrix of these measurements, i.e., ${}^R\mathbf{P}_{0|0} = \mathbf{R}_0$. The initial value of the Riccati recursion is the covariance matrix for the dual-map filter that arises after duplicating the initial state and performing one propagation step. Thus it is equal to:

$$\mathbf{P}_0 = \begin{bmatrix} \mathbf{R}_0 + {}^R\mathbf{Q}_0 & \mathbf{R}_0 \\ \mathbf{R}_0 & \mathbf{R}_0 \end{bmatrix} \quad (18)$$

C. Upper bounds on the Asymptotic Covariance

Having determined the Riccati recursion (Eq. (17)) and its initial value (Eq. (18)), we are now able to derive an upper bound for its solution, and thus an upper bound on the covariance of the map in SLAM. For this purpose, we employ the following lemma:

Lemma 3.1: If \mathbf{R}_u and \mathbf{Q}_u are constant matrices such that $\mathbf{R}_u \succeq \mathbf{R}_k$ and $\mathbf{Q}_u \succeq {}^R\mathbf{Q}_k$, for all $k \geq 1$, then the solution to the Riccati recursion

$$\begin{aligned}\mathbf{P}_{k+1}^u &= \Phi_k \left(\mathbf{P}_k^u - \mathbf{P}_k^u \mathbf{H}^T (\mathbf{H} \mathbf{P}_k^u \mathbf{H}^T + \mathbf{R}_u)^{-1} \mathbf{H} \mathbf{P}_k^u \right) \Phi_k^T \\ &\quad + \mathbf{G} \mathbf{Q}_u \mathbf{G}^T\end{aligned}\quad (19)$$

with an initial condition \mathbf{P}_0^u such that $\mathbf{P}_0^u \succeq \mathbf{P}_0$, satisfies $\mathbf{P}_k^u \succeq \mathbf{P}_k$ for all $k \geq 0$.

The proof of this lemma is based on induction, and employs the fact that the right hand side of the Riccati recursion is a matrix-increasing function of the arguments \mathbf{R}_k and ${}^R\mathbf{Q}_k$. Due to space limitations, the details of the proof are omitted, and the interested reader is referred to [19] for the details of the proof.

We now show how upper bounds on the matrices ${}^R\mathbf{Q}_k$, \mathbf{R}_k , and \mathbf{P}_0 can be derived. From Eqs. (9) and (11) we obtain:

$$\text{trace } {}^R\mathbf{Q}_k = \text{trace } ({}^R\mathbf{G}_k \mathbf{Q} {}^R\mathbf{G}_k^T) = N \sigma_v^2 \delta t^2 + \sigma_w^2 \delta t^2 \sum_{i=1}^N \rho_i^2$$

where ρ_i is the distance of the i -th landmark to the robot. Thus, if ρ_o is the maximum possible distance between the robot

and any landmark (determined, for example, by the robot's maximum sensing range), the following inequality holds:

$$\text{trace } {}^R\mathbf{Q}_k \leq N\sigma_v^2\delta t^2 + N\sigma_\omega^2\rho_o^2\delta t^2 = q$$

We therefore obtain an upper bound for ${}^R\mathbf{Q}_k$, as:

$${}^R\mathbf{Q}_k \preceq qI_{2N} = \mathbf{Q}_u \quad (20)$$

We should note at this point that this is *not* the lowest upper bound that can be derived for ${}^R\mathbf{Q}_k$. By considering the effect of the errors in the translational and rotational velocity measurements separately, a tighter bound can be obtained. The resulting matrix is non-diagonal in this case, however, and this complicates the ensuing analysis. All the pertinent quantities can still be derived in closed form, but the resulting expressions are considerably more cumbersome. We have thus opted not to present the tighter, but more complex bounds in this paper, in the interest of clarity. These results can be found in [19].

An upper bound on the measurement covariance matrix, \mathbf{R}_k , can be derived by considering the characteristics of the particular sensor used for the relative position measurements. If the covariance matrix of the measurement of each individual landmark can be bounded above by $R_{i_k} \preceq rI_2$, then we obtain

$$\mathbf{R}_k \preceq rI_{2N} = \mathbf{R}_u$$

Regarding the initial value of the recursion in Eq. (19), it is easy to see that the following matrix satisfies the condition $\mathbf{P}_0^u \succeq \mathbf{P}_0$:

$$\mathbf{P}_0^u = \begin{bmatrix} (q+r)I_{2N} & rI_{2N} \\ rI_{2N} & rI_{2N} \end{bmatrix} \quad (21)$$

An additional difficulty in solving for the steady-state value of the Riccati recursion in Eq. (19) is that the state transition matrix, Φ_k , is time-varying. Considering, however, the special structure of the matrices that appear in this recursion, the following lemma can be proven [19]:

Lemma 3.2: Let the solution, \mathbf{P}_k^u , to the recursion in Eq. (19) be partitioned in $2N \times 2N$ blocks as

$$\mathbf{P}_k^u = \begin{bmatrix} {}^R\mathbf{P}_k^u & \mathbf{P}_{RG_k} \\ \mathbf{P}_{RG_k}^T & G\mathbf{P}_k^u \end{bmatrix} \quad (22)$$

Additionally, let $\bar{\mathbf{P}}_k$ be the solution to the recursion

$$\bar{\mathbf{P}}_{k+1} = \bar{\mathbf{P}}_k - \bar{\mathbf{P}}_k \mathbf{H}^T (\mathbf{H}\bar{\mathbf{P}}_k \mathbf{H}^T + \mathbf{R}_u)^{-1} \mathbf{H}\bar{\mathbf{P}}_k + \mathbf{G}\mathbf{Q}_u \mathbf{G}^T \quad (23)$$

with initial condition $\bar{\mathbf{P}}_0 = \mathbf{P}_0^u$, and let $\bar{\mathbf{P}}_k$ be partitioned as

$$\bar{\mathbf{P}}_k = \begin{bmatrix} {}^R\bar{\mathbf{P}}_k & \bar{\mathbf{P}}_{RG_k} \\ \bar{\mathbf{P}}_{RG_k}^T & G\bar{\mathbf{P}}_k \end{bmatrix} \quad (24)$$

Then for any $k \geq 0$, the following relations hold:

$${}^R\bar{\mathbf{P}}_k = {}^R\mathbf{P}_k^u, \quad G\bar{\mathbf{P}}_k = G\mathbf{P}_k^u, \quad \text{and} \quad \mathbf{P}_{RG_k} = \mathbf{C}_k \bar{\mathbf{P}}_{RG_k}$$

where $\mathbf{C}_k = \prod_{i=1}^k {}^R\Phi_k$.

This lemma demonstrates that to derive an upper bound on the steady-state covariance of the absolute and relative maps

in SLAM, it suffices to determine the steady-state solution of the Riccati in Eq. (23). This recursion is simpler than that of Eq. (19), since it is a *constant coefficient* Riccati recursion. In order to determine the *asymptotic* solution of Eq. (23), we employ the following lemma, which has been adapted from [20]:

Lemma 3.3: Suppose $\bar{\mathbf{P}}_k^{u(0)}$ is the solution to the discrete-time Riccati recursion in Eq. (23) with initial value $\mathbf{P}_0^u = \mathbf{0}_{4N \times 4N}$. Then the solution with the initial condition given in Eq. (21) is determined by the identity

$$\bar{\mathbf{P}}_k^u - \bar{\mathbf{P}}_k^{u(0)} = \mathbf{T}_k (I_{4N} + \bar{\mathbf{P}}_0 \mathbf{J}_k)^{-1} \bar{\mathbf{P}}_0 \mathbf{T}_k^T$$

where \mathbf{T}_k is given by

$$\mathbf{T}_k = (I_{4N} - \mathbf{K}_p \mathbf{H})^k (I_{4N} + \mathbf{P} \mathbf{J}_k)$$

In these expressions, \mathbf{P} is any solution to the Discrete Algebraic Riccati Equation (DARE):

$$\mathbf{P} = \mathbf{P} - \mathbf{P} \mathbf{H}^T (\mathbf{H} \mathbf{P} \mathbf{H}^T + \mathbf{R}_u)^{-1} \mathbf{H} \mathbf{P} + \mathbf{G} \mathbf{Q}_u \mathbf{G}^T$$

and $\mathbf{K}_p = \mathbf{P} \mathbf{H}^T (\mathbf{H} \mathbf{P} \mathbf{H}^T + \mathbf{R}_u)^{-1}$. \mathbf{J}_k denotes the solution to the *dual* Riccati recursion:

$$\mathbf{J}_{k+1} = \mathbf{J}_k - \mathbf{J}_k \mathbf{G} (\mathbf{G}^T \mathbf{J}_k \mathbf{G} + \mathbf{Q}_u^{-1})^{-1} \mathbf{G}^T \mathbf{J}_k + \mathbf{H}^T \mathbf{R}_u^{-1} \mathbf{H}$$

with zero initial condition, $\mathbf{J}_0 = \mathbf{0}_{4N \times 4N}$.

Lemma 3.3 simplifies the evaluation of the steady-state value of $\bar{\mathbf{P}}_k$, since the solution to the Riccati recursion with zero initial condition is easily derived. When the initial value of the covariance is zero, then the submatrix of $\bar{\mathbf{P}}_k$ that corresponds to the covariance of the absolute map will *remain* zero for all $k \geq 0$, since no influx of uncertainty occurs in the absolute landmark coordinates. This observation results in significant simplification of the necessary derivations, which are presented in detail in [19].

Applying Lemmas 3.3 and 3.2, and evaluating the limit of the resulting expressions as $k \rightarrow \infty$, allows us to obtain the following upper bound for the asymptotic covariance matrix of the augmented-state filter:

$$\mathbf{P}_\infty \preceq \begin{bmatrix} \left(\frac{q}{2} + \sqrt{\frac{q^2}{4} + qr} \right) I_{2N} & \mathbf{0}_{2N \times 2N} \\ \mathbf{0}_{2N \times 2N} & \left(-\frac{q}{2} + \sqrt{\frac{q^2}{4} + qr} \right) I_{2N} \end{bmatrix}$$

This expression provides an upper bound for the covariance of the augmented state vector after every EKF *propagation* step. To derive a bound for the covariance immediately after the *update* step of the EKF, we note that during propagation, the absolute map covariance remains unchanged, while the uncertainty of the relative map is increased according to Eq. (10). Using this observation, we can show that an upper bound on the steady-state covariance matrix of the relative map, immediately after every update step, is given by

$${}^R\bar{\mathbf{P}}_\infty = \left(-\frac{q}{2} + \sqrt{\frac{q^2}{4} + qr} \right) I_{2N} = r_{\text{map}} I_{2N} \quad (25)$$

while the asymptotic uncertainty of the absolute positions of the landmarks in SLAM is bounded above by the matrix

$${}^G\bar{\mathbf{P}}_\infty = \left(-\frac{q}{2} + \sqrt{\frac{q^2}{4} + qr} \right) I_{2N} = r_{\text{map}} I_{2N} \quad (26)$$

These results provide bounds for the accuracy of the map in SLAM, which are evaluated in closed form, and depend on the accuracy of the robot's sensors, as well as on the size of the area being mapped. Interestingly, the *bounds* on both the relative and absolute map are *equal*, when the covariance matrix after the update phase of the EKF is considered. However, it should be clear that the *actual* covariance matrices of the two map representations are *not* identical at steady state. In the next section, we show how these results can be used for obtaining bounds on the covariance of the robot's pose estimates in SLAM.

IV. THE ACCURACY OF POSE ESTIMATION IN SLAM

Although the robot pose (position and orientation) is not explicitly contained in the state vector of the formulation that we presented in the preceding section, an estimate for this pose is implicitly defined from the estimates of the relative map, ${}^R\mathbf{X}$, and the absolute map, ${}^G\mathbf{X}$. Specifically, the relation between the representation of the i -th landmark in the global frame, ${}^G p_i$, and in the robot frame at time step k , ${}^{R_k} p_i$, is given by:

$${}^G p_i = {}^G p_{R_k} + C(\phi_k) {}^{R_k} p_i \quad (27)$$

where ${}^G p_{R_k}$ and ϕ_k are the position and orientation of the robot with respect to the global frame at time step k , respectively. Thus, given the augmented state vector at time-step k , $\mathbf{X}_k = [{}^R\mathbf{X}^T \quad {}^G\mathbf{X}^T]^T$, and its covariance, \mathbf{P}_k , we are able to determine the robot pose,

$$\boldsymbol{\theta}_k = [{}^G p_{R_k}^T \quad \phi_k^T]^T$$

and its covariance, $\mathbf{P}_{\boldsymbol{\theta}\boldsymbol{\theta}}$, by solving the Least Squares minimization problem:

$$\min_{\boldsymbol{\theta}_k} \boldsymbol{\varepsilon}_k^T \mathbf{W}_k^{-1} \boldsymbol{\varepsilon}_k \quad (28)$$

where $\boldsymbol{\varepsilon}_k$ is the vector of errors that we seek to minimize, i.e., the $2N \times 1$ vector whose i -th block is equal to

$$\boldsymbol{\varepsilon}_i = {}^G p_{R_k} + C(\phi_k) {}^{R_k} p_i - {}^G p_i \quad (29)$$

and \mathbf{W}_k is the covariance matrix of the vector $\boldsymbol{\varepsilon}_k$. Employing linearization of Eq. (29), we obtain

$$\mathbf{W}_k = \mathbf{H}_{X_k} \mathbf{P}_k \mathbf{H}_{X_k}^T \quad (30)$$

where \mathbf{H}_{X_k} is the Jacobian of the error vector $\boldsymbol{\varepsilon}_k$ with respect to the state vector \mathbf{X}_k , given by

$$\mathbf{H}_{X_k} = [I_N \otimes C(\phi_k) \quad I_{2N}] \quad (31)$$

The covariance matrix of the least-squares estimate for $\boldsymbol{\theta}_k$ is:

$$\begin{aligned} \mathbf{P}_{\boldsymbol{\theta}\boldsymbol{\theta}} &= (\mathbf{H}_{\boldsymbol{\theta}_k}^T \mathbf{W}_k^{-1} \mathbf{H}_{\boldsymbol{\theta}_k})^{-1} \\ &= \left(\mathbf{H}_{\boldsymbol{\theta}_k}^T (\mathbf{H}_{X_k} \mathbf{P}_k \mathbf{H}_{X_k}^T)^{-1} \mathbf{H}_{\boldsymbol{\theta}_k} \right)^{-1} \end{aligned} \quad (32)$$

where $\mathbf{H}_{\boldsymbol{\theta}_k}$ is the Jacobian matrix of the error vector $\boldsymbol{\varepsilon}_k$ with respect to $\boldsymbol{\theta}_k$. This is a $2N \times 3$ block matrix, whose i -th block element is equal to

$$H_i = [I_2 \quad \check{p}_{i_k}], \quad \text{with } \check{p}_{i_k} = -J_{\times} C(\phi_k) {}^{R_k} p_i \quad (33)$$

We point out that the solution of the Least Squares problem in Eq. (28) and the covariance of this solution, given by Eq. (32), yield the *same* results for the robot's pose, as the "standard" EKF formulation for SLAM, when at least 2 landmarks are available. This is because in both cases, *all* the available measurements are used, and no approximations are made (apart from linearization). Thus, we can use the expression of Eq. (32), to study the properties of the robot's pose covariance in EKF-based SLAM.

In the following, we focus on deriving upper bounds on the steady-state value of the matrix $\mathbf{P}_{\boldsymbol{\theta}\boldsymbol{\theta}}$. Note that since $\mathbf{P}_k \preceq \mathbf{P}_k^u$, an upper bound for the covariance of the robot pose at time-step k is given by (cf. Eq. (32)):

$$\mathbf{P}_{\boldsymbol{\theta}\boldsymbol{\theta}}^u = \left(\mathbf{H}_{\boldsymbol{\theta}_k}^T (\mathbf{H}_{X_k} \mathbf{P}_k^u \mathbf{H}_{X_k}^T)^{-1} \mathbf{H}_{\boldsymbol{\theta}_k} \right)^{-1} \quad (34)$$

Substitution of the asymptotic results from Eqs. (25) and (26), and of the values of the Jacobians $\mathbf{H}_{\boldsymbol{\theta}_k}$ and \mathbf{H}_{X_k} from Eqs. (31) and (33), yields the following asymptotic value for $\mathbf{P}_{\boldsymbol{\theta}\boldsymbol{\theta}}^u$:

$$\mathbf{P}_{\boldsymbol{\theta}\boldsymbol{\theta}}^u = 2r_{\text{map}} \begin{bmatrix} NI_2 & \sum_{i=1}^N \check{p}_i \\ \sum_{i=1}^N \check{p}_i^T & \sum_{i=1}^N (\check{p}_i^T \check{p}_i) \end{bmatrix}^{-1} = \begin{bmatrix} P_{PP} & P_{P\phi} \\ P_{P\phi}^T & P_{\phi\phi} \end{bmatrix} \quad (35)$$

Employing inversion of the partitioned matrix in Eq. (35) we obtain the following expression for $P_{\phi\phi}$:

$$P_{\phi\phi} = \frac{2r_{\text{map}}}{\sum_{i=1}^N (\check{p}_i^T \check{p}_i) - \frac{1}{N} \left(\sum_{i=1}^N \check{p}_i^T \right) \left(\sum_{i=1}^N \check{p}_i \right)} \quad (36)$$

Noting that for any i, j , the property $\check{p}_i^T \check{p}_j = {}^R p_i^T {}^R p_j$ holds, and after simple algebraic manipulation, we can re-write the expression for $P_{\phi\phi}$ as [19]:

$$P_{\phi\phi} = \frac{4Nr_{\text{map}}}{\sum_{i=1}^N \sum_{j=1}^N \rho_{ij}^2} \quad (37)$$

where ρ_{ij} is the distance between landmarks i and j . Thus, if the pairwise distances of the landmarks are known, an upper bound on the robot's orientation variance is determined by the preceding expression. Furthermore, if some properties of the placement of the landmarks in space is known, using this expression we can determine bounds that are independent of the *actual* landmark positions. For example, if the minimum allowable distance between any two landmarks is equal to $\rho_{LL\min}$, then

$$P_{\phi\phi} \leq \frac{4r_{\text{map}}}{(N-1)\rho_{LL\min}^2} \quad (38)$$

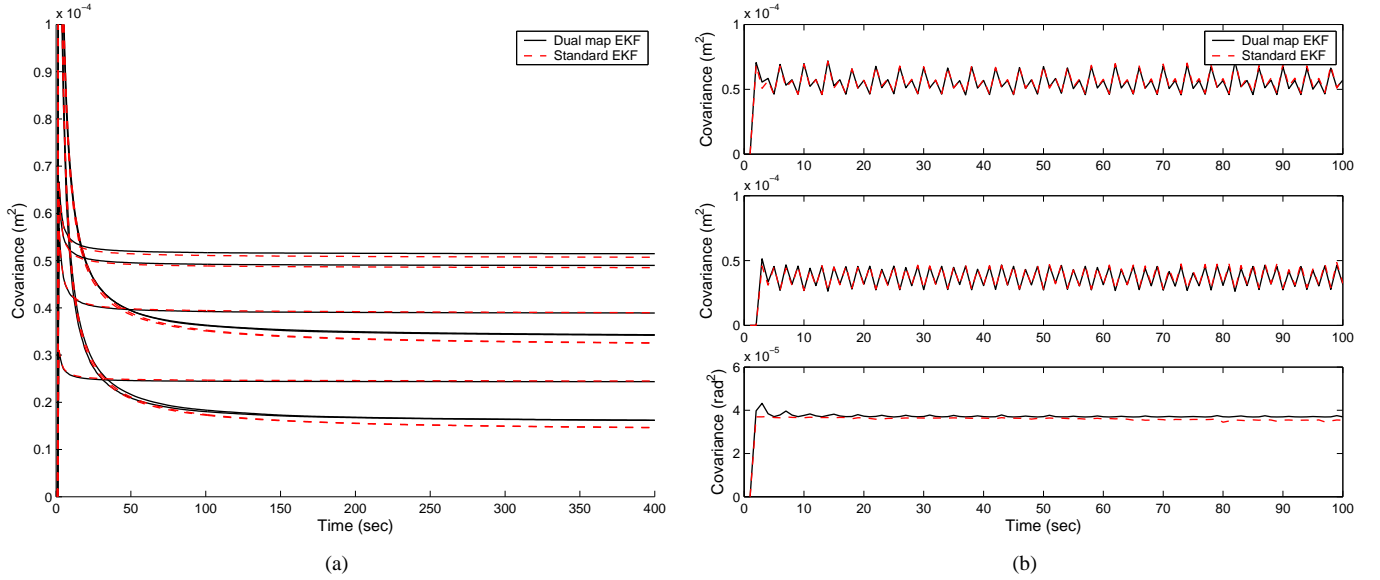


Fig. 1. (a) The diagonal elements of the covariance of the landmark position estimates, computed by the standard EKF SLAM algorithm, and by the dual-map filter presented in Section III. (b) The diagonal elements of the robot pose covariance, computed by the standard EKF SLAM algorithm, and by the method described in Section IV. To preserve the clarity of the figure, only the first 100sec are shown.

For the upper bound on the covariance matrix of the robot's position estimates, we obtain from Eq. (35):

$$P_{PP} = 2r_{\text{map}} \left(NI_2 - \frac{\left(\sum_{i=1}^N \check{p}_i \right) \left(\sum_{i=1}^N \check{p}_i^T \right)}{\sum_{i=1}^N \left(\check{p}_i^T \check{p}_i \right)} \right)^{-1}$$

which, by application of the matrix inversion lemma, yields:

$$P_{PP} = \frac{2r_{\text{map}}}{N} I_2 + \underbrace{\frac{2r_{\text{map}} \left(\sum_{i=1}^N \check{p}_i \right) \left(\sum_{i=1}^N \check{p}_i^T \right)}{N^2 \left(\sum_{i=1}^N \left(\check{p}_i^T \check{p}_i \right) - \frac{1}{N} \left(\sum_{i=1}^N \check{p}_i^T \right) \left(\sum_{i=1}^N \check{p}_i \right) \right)}}_{T_2}$$

To derive an upper bound for P_{PP} , we examine the trace of the second term, T_2 , in the last expression. After some algebraic manipulation, it can be shown that

$$\text{trace}(T_2) = \frac{4r_{\text{map}} \sum_{i=1}^N \left(R p_i^T R p_i \right)}{\sum_{i=1}^N \sum_{j=1}^N \rho_{ij}^2} - \frac{2r_{\text{map}}}{N}$$

and thus

$$P_{PP} \preceq \frac{2r_{\text{map}}}{N} I_2 + \text{trace}(T_2) I_2 = \frac{1}{N} P_{\phi\phi} \sum_{i=1}^N \rho_i^2 I_2$$

Finally, we observe that if the maximum distance between the robot and any landmark is equal to ρ_o , the covariance of the robot's position estimate is bounded above by

$$P_{PP} \preceq \rho_o^2 P_{\phi\phi} I_2 \quad (39)$$

This result, along with those of Eqs. (37)-(38), which determine upper bounds on the robot's orientation uncertainty, and that of Eq. (26), which yields the upper bound of the

covariance matrix of the global landmark coordinates, are the most important results of this paper. They enable us to compute the *guaranteed accuracy* of the state estimates in SLAM, as an *analytical function* of the accuracy of the robot's sensors, and the properties of the landmarks' configuration. Hence, these expressions can be employed to determine whether a candidate robot system design satisfies the accuracy requirements of a given SLAM application, *without* the need for simulations, or experimentation.

For example, consider a scenario in which a service robot (e.g., autonomous lawn-mower, autonomous vacuum-cleaner) is operating in an area of approximately known size, and localizes by performing SLAM. Clearly, the state vector should contain as few landmarks as possible, to minimize the computational requirements of the localization algorithm. Moreover, the robot's sensors should be as inexpensive (and thus, as inaccurate) as possible, in order to minimize production costs. By employing the results of this paper during the design phase, the trade-offs between cost, complexity, and localization accuracy can be studied, and informed decisions can be reached. Moreover, during the robot's operation, the selection of landmarks to include in the state vector can be guided by the results of Eqs. (37)-(38), to ensure *theoretical guarantees* for the robot's pose accuracy. It thus becomes clear that the availability of closed-form expressions that characterize the accuracy of the state estimates in SLAM is a powerful tool, which can be employed both in the design phase and during the operation of robotic systems. In the following section, we present results from real-world experiments, which demonstrate the validity of the preceding theoretical analysis.

V. EXPERIMENTAL RESULTS

Before describing the setup of our real-world experiments, we illustrate, with numerical results, that the dual map formu-

lation employed in our analysis is equivalent to the “standard” EKF SLAM formulation, in which the state vector comprises the robot pose and the landmark positions. For this purpose, we consider a SLAM scenario in which a robot moves randomly in a square area of side 4m, and observes four landmarks randomly placed in the area. Both the “standard” EKF-based SLAM algorithm, and the one described in Section III, process the same data, and the results for the covariance of the global landmark coordinates are shown in Fig. 1(a). In this plot we observe that the numerical results obtained with both filters are almost identical, with only small differences due to linearization and numerical errors. Moreover, in Fig. 1(b) we plot the diagonal elements of the robot’s pose covariance matrix, computed both by the standard EKF SLAM, and using Eq. (32). Once again, we observe that the two methods yield almost identical results, thus indicating that by studying the properties of the covariance in our formulation, we can draw conclusions for the covariance in the standard EKF-based SLAM algorithm.³

In our real-world experiments, a Pioneer 3 robot equipped with two opposite-facing SICK LMS200 laser scanners, which provide a 360° field of view, was employed (cf. Fig. 2(a)). During the experiment presented in this paper, the robot moves randomly while performing SLAM in an area of approximate dimensions 10m×4m. The laser scans are processed for detecting four prominent corners in the area, which are used as landmarks. For detecting each corner, line-fitting is employed to compute the equations of adjacent wall lines, and the intersection of these lines is determined. The maximum standard deviation of each of the robot-to-landmark measurements was experimentally found to be equal to approximately 0.15m, which yields an upper bound $R \preceq 0.0225I_2m^2$. The robot receives translational velocity measurements with standard deviation $\sigma_v = 0.01m/sec$, and rotational velocity measurements with $\sigma_\omega = 5 \times 10^{-3}rad/sec$. The estimated robot trajectory, as well as the landmark positions, are shown in Fig. 2(b). In the same figure, a sample laser scan is superimposed (after being transformed to the global frame), to illustrate the geometry of the area where the robot operates.

In Fig. 3, the standard deviation of the estimation errors (solid lines), as this is computed by the filter, is compared to the standard deviation computed with the theoretically derived bounds (dashed lines). For the robot orientation, the bound in Eq. (38) is employed in this case. From the plots in Fig. 3, we conclude that the analytical bounds that we have derived can be employed in order to *predict* the localization accuracy of SLAM without having to resort to extensive simulations, or experimentation.

We should point out that in this particular case, where the robot moves randomly in space, the actual standard deviations are approximately 2-3 times smaller than the corresponding upper bounds. If the robot’s trajectory was such that the robot-

to-landmark distances were always close to their maximum values, the bounds would have been significantly tighter. This fact has been verified in numerous simulation studies of “adverse” SLAM setups. Finally, it is worth mentioning that due to occlusions and data association failures, the landmarks were not detected in every laser scan. On the average, the landmarks were successfully detected 94% of the time. Despite these fluctuations in the number of observed landmarks, the theoretical bounds still provide a quite accurate characterization of the uncertainty in SLAM.

VI. CONCLUSIONS

In this paper, we have derived upper bounds on the covariance of the state estimates in SLAM, as *analytical* functions of the accuracy of the robot’s sensors, and of the properties of the map (e.g., number of landmarks, maximum distance to landmarks). These bounds determine the *guaranteed accuracy* that will be attained by a robot with a given set of sensors, performing SLAM. Therefore, they can be used during the design of a localization system, to guide the selection of important parameters that affect the system’s performance, cost, and algorithmic complexity. The derived analytical expressions simplify the process of verifying whether a particular design meets the accuracy requirements of a given application, minimizing the need for tedious and time-consuming simulation studies, or exhaustive experimentation. In our future work, we plan to extend these results to cases in which the robot does not operate within the same area for its entire mission. In such cases, the number of visible landmarks dynamically changes over time, and important issues such as loop-closure arise. In this case, the length of the loops of the environment is a crucial factor, which determines the accuracy of the robot’s localization. We believe that the theoretical analysis presented in this paper can serve as a basis for the study of more complex SLAM scenarios.

ACKNOWLEDGEMENTS

This work was supported by the University of Minnesota (GiA Award, DTC), the Jet Propulsion Laboratory (Grant No. 1248696, 1251073), and the National Science Foundation (ITR, Grant No. EIA-0324864).

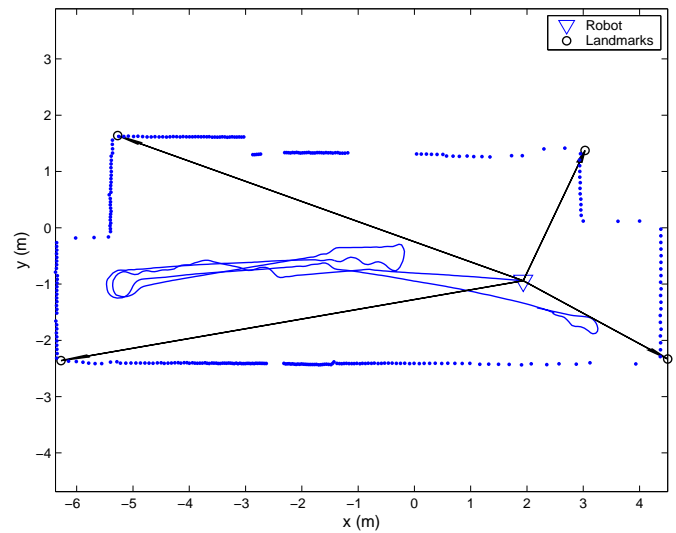
REFERENCES

- [1] M. Montemerlo, “FastSLAM: A factored solution to the simultaneous localization and mapping problem with unknown data association,” Ph.D. dissertation, Robotics Institute, Carnegie Mellon University, 2003.
- [2] P. Newman, J. Leonard, J. D. Tardos, and J. Neira, “Explore and return: experimental validation of real-time concurrent mapping and localization,” in *Proc. of the IEEE International Conference on Robotics and Automation*, Washington, DC, May 11-15 2002, pp. 1802–9.
- [3] S. B. Williams, G. Dissanayake, and H. Durrant-Whyte, “An efficient approach to the simultaneous localisation and mapping problem,” in *Proc. of the 2002 IEEE International Conference on Robotics and Automation*, Washington, DC, May 11-15 2002, pp. 406–11.
- [4] S. Thrun, Y. Liu, D. Koller, A. Ng, Z. Ghahramani, and H. Durrant-Whyte, “Simultaneous localization and mapping with sparse extended information filters,” *International Journal of Robotics Research*, vol. 23, no. 7-8, pp. 693–716, Aug. 2004.
- [5] M. Paskin, “Thin junction tree filters for simultaneous localization and mapping,” Ph.D. dissertation, Berkeley, 2002.

³We should note that the estimates for the robot’s pose and for the landmarks’ positions computed by the two methods are also practically identical, and the dual-map filter is consistent. The corresponding plots are not included, due to limited space.

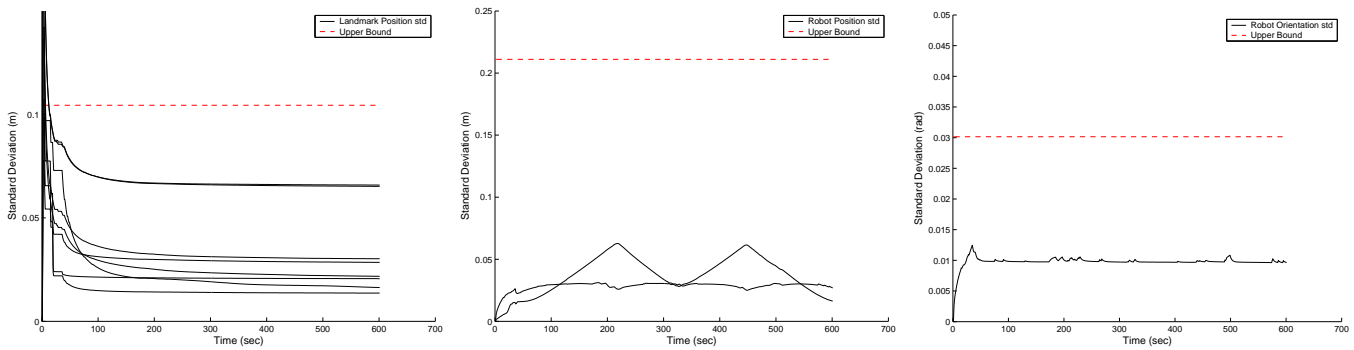


(a)



(b)

Fig. 2. (a) The Pioneer 3 robot used in the real-world experiments. (b) The estimated robot trajectory and landmark positions, superimposed on a sample laser scan from the area where the robot moves. The arrows indicate the robot-to-landmark measurements.



(a)

(b)

(c)

Fig. 3. (a) The landmarks' position standard deviation and corresponding upper bound (b) The robot's position standard deviation and corresponding upper bound (c) The robot's orientation standard deviation and corresponding upper bound

[6] J. Neira and J. D. Tardos, "Data association in stochastic mapping using the joint compatibility test," *IEEE Transactions on Robotics and Automation*, vol. 17, no. 6, pp. 890–897, 2001.

[7] S. Se, D. G. Lowe, and J. Little, "Mobile robot localization and mapping with uncertainty using scale-invariant visual landmarks," *International Journal of Robotics Research*, vol. 21, no. 8, pp. 735–758, 2002.

[8] F. Tang, M. Adams, J. Ibanez-Guzman, and S. Wijesoma, "Pose invariant, robust feature extraction from range data with a modified scale space approach," in *Proc. of the IEEE International Conference on Robotics and Automation*, New Orleans, LA, Apr 26–May 1 2004, pp. 3173–3179.

[9] A. I. Mourikis and S. I. Roumeliotis, "Analysis of positioning uncertainty in simultaneous localization and mapping (SLAM)," in *Proc. of the IEEE/RSJ International Conference on Robotics and Intelligent Systems (IROS)*, Sendai, Japan, September 28 - October 2 2004, pp. 13–20.

[10] —, "Performance bounds for cooperative simultaneous localization and mapping (C-SLAM)," in *Proc. of Robotics: Science and Systems Conference*, Cambridge, MA, June 8–11 2005, pp. 73–80.

[11] P. W. Gibbens, G. M. W. M. Dissanayake, and H. F. Durrant-Whyte, "A Closed Form Solution to the Single Degree of Freedom Simultaneous Localisation and Map Building (SLAM) Problem," in *Proceedings of the 39th IEEE Conference on Decision and Control*, Sydney, NSW, Australia, 12–15 December 2000, pp. 191–196.

[12] E. W. Nettleton, P. W. Gibbens, and H. F. Durrant-Whyte, "Closed form solutions to the multiple platform simultaneous localization and map building (SLAM) problem," in *Sensor Fusion: Architectures, Algorithms, and Applications IV*, B. V. Dasarthy, Ed., vol. 4051, Bellingham, WA, 2000, pp. 428–437.

[13] P. M. Newman, "On the Structure and Solution of the Simultaneous Localisation and Map Building Problem," Ph.D. dissertation, University of Sydney, March 1999.

[14] M. Csorba, "Simultaneous Localization and Map Building," Ph.D. dissertation, University of Oxford, 1997.

[15] G. M. W. M. Dissanayake, P. M. Newman, H. F. Durrant-Whyte, S. Clark, and M. Csorba, "A Solution to the Simultaneous Localization and Map Building (SLAM) Problem," *IEEE Transactions of Robotics and Automation*, vol. 17, no. 3, pp. 229–241, June 2001.

[16] J. W. Fenwick, P. M. Newman, and J. J. Leonard, "Cooperative Concurrent Mapping and Localization," in *Proceedings of the 2002 IEEE International Conference on Robotics and Automation*, Washington D.C., 11–15 May 2002, pp. 1810–1817.

[17] J. W. Fenwick, "Collaborative Concurrent Mapping and Localization," Master's thesis, Massachusetts Institute of Technology, June 2001.

[18] R. C. Smith, M. Self, and P. Cheeseman, *Autonomous Robot Vehicles*. Springer-Verlag, 1990, ch. Estimating Uncertain Spatial Relationships in Robotics, pp. 167–193.

[19] A. I. Mourikis and S. I. Roumeliotis, "Analytical characterization of the accuracy of SLAM without absolute orientation measurements," University of Minnesota, Dept. of Computer Science and Engineering, Tech. Rep., 2006.

[20] B. Hassibi, "Indefinite metric spaces in estimation, control and adaptive filtering," Ph.D. dissertation, Stanford University, August 1996.